Spectrochimica Acta Part A: Molecular and Biomolecular Spectroscopy 217 (2019) 271–277

Contents lists available at ScienceDirect

Spectrochimica Acta Part A: Molecular and Biomolecular Spectroscopy

journal homepage: www.elsevier.com/locate/saa

Novel electrochemical sensor based on molecularly imprinted polymer for selective recognition of sesquiterpene β-caryophyllene

Igor Medeiros de Assis [a], Maria Oneide Silva de Moraes [a], Relem Cativo da Conceição [a], Yonny Romaguera-Barcelay [b], Rodrigo Fernando Brambilla de Souza [d], Dunieskys Roberto González Larrudé [e], Maria Luiza Miranda Rocco [c], Walter Ricardo Brito [a,*]

[a] Department of Chemistry, Federal University of Amazonas, Manaus, Amazonas 69067-005, Brazil
[b] Department of Physics, Federal University of Amazonas, Manaus, Amazonas 69067-005, Brazil
[c] Institute of Chemistry, Federal University of Rio de Janeiro, Rio de Janeiro, Rio de Janeiro 21941-901, Brazil
[d] Instituto de Pesquisas Energéticas e Nucleares, Av. Prof. Lineu Prestes, 2242, 05508-000, Butantã, São Paulo, SP, Brazil
[e] MackGraphe, Universidade Presbiteriana Mackenzie, Rua da Consolação 896, Consolação, 01302-907 São Paulo, SP, Brazil

ARTICLE INFO

Article history:
Received 20 November 2018
Received in revised form 26 March 2019
Accepted 28 March 2019
Available online 29 March 2019

Keywords:
β-Caryophyllene
MIP
Carbon paste electrode
Electrochemical sensor

ABSTRACT

Molecularly imprinted polymers provide an excellent platform for the modification of selective electrodes for sensing applications. Herein, we present a novel modified carbon paste electrode (CPE) with a selective molecularly imprinted polymer (MIP) for recognition of sesquiterpene β-caryophyllene, constituted of important plants oil-resins and extracts. The non-covalent MIP was synthesized using AA, EGDMA, and AIBN as a functional monomer, cross-linker and initiator agent, respectively. Structural and chemical characterization of the synthesized MIP was conducted through scanning electron microscopy (SEM), Fourier-transform infrared (FT-IR) spectroscopy, Raman spectroscopy and X-ray photoelectron spectroscopy (XPS). It was possible to verify the functional features of the synthesized MIP related to the extraction process of the template molecule. The CPE modified with MIP for sesquiterpene β-caryophyllene recognition was characterized by electrochemical techniques as cyclic voltammetry (CV) and square wave voltammetry (SWV). The highest selective recognition electrode enables to detect concentrations in the range between 1.5×10^{-7} and 7.5×10^{-7} M, showing great potential for applications in monitoring content of sesquiterpene β-caryophyllene in technological processes and for predicting the quality of extracts, oils, and resins of plants.

1. Introduction

The sesquiterpene β-caryophyllene is a bicyclic compound present in several plant extracts, oils and resins [1,2]. β-Caryophyllene is widely used as a flavoring agent and additive in food and cosmetics applications [3,4]. The pharmaceutical industry uses the β-caryophyllene due to its potentialized effect as anesthetic, antifungal, antiviral, spasmolytic and anti-inflammatory [5–8].

Among the diverse applications of β-caryophyllene stands out their extensive use as an herbal medicine that requires rigorous quality control when extracted from the natural source raw material. On the other hand, the extraction of β-caryophyllene isn't trivial. Pharmaceutical and cosmetic industries make their products using original vegetable extracts and oil resins and these raw materials are complex mixtures formed by a large number of compound requiring specific techniques and reagents for extraction and identification [9,10],β-caryophyllene is usually obtained using chromatographic methods and their identification through expensive analytical techniques [11,12].

Molecularly imprinted polymers (MIP's) are materials with highly selective cavities that act as specific detectors or molecular sieves, which can help to identify β-caryophyllene from the plant extracts. MIP's have been widely used in the chromatographic separation, capillary electrophoresis, selective extraction, solid phase microextraction and as electrochemical sensors [13,14]. The application of MIP's as electrochemical sensor for β-caryophyllene can offer high performance in selective detection of this compound with important technological applications [15–17].

In this work it is presented a novel electrochemical sensor for detection of the β-caryophyllene based on CPE modified with MIP. The synthesized MIP was characterized by different techniques for deepening into its behavior and functionality. The electrochemical sensor showed great potential for technological applications in the qualification and control of oils-resins and plant extract, as well as in the cosmetic and pharmaceutical industries that use natural raw materials.

* Corresponding author.
E-mail address: wrbrito@ufam.edu.br (W.R. Brito).

https://doi.org/10.1016/j.saa.2019.03.097
1386-1425/

2. Experimental

2.1. Materials and methods

β-Caryophyllene, acrylic acid (AA), ethylene glycol dimethacrylate (EGDMA), 2,2′-azo-bis-isobutyronitrile (AIBN), methanol and acetonitrile were purchased from Sigma-Aldrich (Steinheim, Germany). All reagents are of analytical grade and have been used without purification. All solutions were prepared using water from a Millipore (Billerica, MA, USA) Milli-Q purification system.

2.2. Synthesis of MIP

The MIP synthesis was performed using the procedure reported by Pardeshi et al. [18]. First, the template molecule β-caryophyllene (1 mmol), and the functional monomer AA (4 mmol) were added to 10 mL of acetonitrile in a glass tube with the screw cap. The cross-linker EGDMA (40 mmol) and the initiator AIBN (0.3 mmol) were then added. The mixture was purged with nitrogen for 10 min before placed to polymerize for 24 h immersed in a 60 °C water bath. The synthesized MIP was macerated in Agatha mortar for 5 min, mixed with methanol and placed in the ultrasonic bath for 15 min; this procedure was repeated to remove the template molecule from the polymeric matrix. Fig. 1. shows the schematic representation of the functioning of MIP before and after template removal.

The non-imprinted polymer (NIP) was synthesized following the same procedure described above without the template.

2.3. Characterization methods

Scanning electron microscopy (SEM) images were obtained by Oxford model X-ACT microscope. For this purpose, the MIP and NIP were sputtered with a layer of gold and the images were observed under a voltage of 25 kV.

FTIR spectra were recorded using a Thermo Electron (model Nicolet S10) spectrophotometer, with 32 scans in the range of 4000 to 400 $cm^{-1}$and a resolution of 4 cm^{-1}. Samples were mixed with KBr in a weight ratio of 1:100 and compressed to obtain a thin film disk for the spectrum analysis.

The active vibrational mode spectra were collected using a Confocal Raman microscope (WITec alpha 300R, WITec GmbH, Ulm, Germany) equipped with a cooled CCD using a 50× magnification lens and 600 g mm^{-1} grating with the integration time of 1 s and 10 accumulations. The samples were excited using a blue laser (wavelength 488 nm, power at 20 mW). The spectra were obtained at room temperature in the spectral range 100–3600 cm^{-1}.

XPS measurements were performed at the ESCALAB 250Xi spectrometer (Thermo Scientific) equipped with an electron energy hemispherical analyzer using monochromatized Al Kα line ($h\upsilon$ = 1486.6 eV) excitation. The spectra were energy referenced to the C1s signal of aliphatic C atoms at the binding energy of 285.00 eV. XPS spectra were collected using X-ray beam spot size = 650 μm with an emission angle of 90° with respect to the sample surface. The powders were placed on conductive double-sided carbon tape and the spectra were collected at two different points of the sample. High-resolution spectra were acquired with 25 eV pass energy at C1s and O1s core levels.

Electrochemical characterization was performed at AUTOLAB® PGSTAT 204 N (Metrohm Autolab) with the NOVA 2.1 with the platinum wire as a counter electrode, Ag/AgCl as a reference electrode, and a commercial CPE (diameter of 3.00 mm, with the cavity of 2 mm depth) as the working electrode.

2.4. Electrode preparation

The modified carbon paste was prepared by the mixture of 0.025 g of carbon black, 0.025 g of MIP after template removal and 0.100 g of bi-component epoxy resin with the addition of 15 μL of cyclohexanone. The resulting paste was then packed firmly into the electrode cavity. The electrodes were left at room temperature for solidification and the excess of solidified material was carefully removed with sandpaper (4000 grit). For comparative studies CPE modified with NIP was prepared following the same procedure.

2.5. Electrochemical characterization

The electrochemical characterization was first performed using the CV technique with potentials between −1 V and 1 V, scan velocity of 25 mV in 10 mL of $K_3[Fe(CN)_6]/K_4[Fe(CN)_6$ (5 mM) and KCl (0.2 M).

For determination of the β-caryophyllene the modified CPE were incubated for 5 min in solutions containing different concentrations of β-caryophyllene followed of the removal of the excess of solution from the electrode surface by immersion for 10 s in methanol. The electrochemical measurement was conducted using the SWV technique with the following parameters: scanning potential from −0.1 to 0.7 V, modulation amplitude 0.02 V, step 0.005 V and frequency 25 Hz. The measurements were performed in 10 mL of $K_3[Fe(CN)_6]/K_4[Fe(CN)_6$(5 mM) and KCl (0.2 M).

3. Results and discussion

3.1. Scanning electron microscopy studies

The SEM exploration has been performed to understand the morphological modifications of the synthesized MIP and NIP. Fig. 2 shows morphological differences between the NIP (a) and MIP after template removal (b). Fig. 2a) exhibits a smooth, and continuous surface with

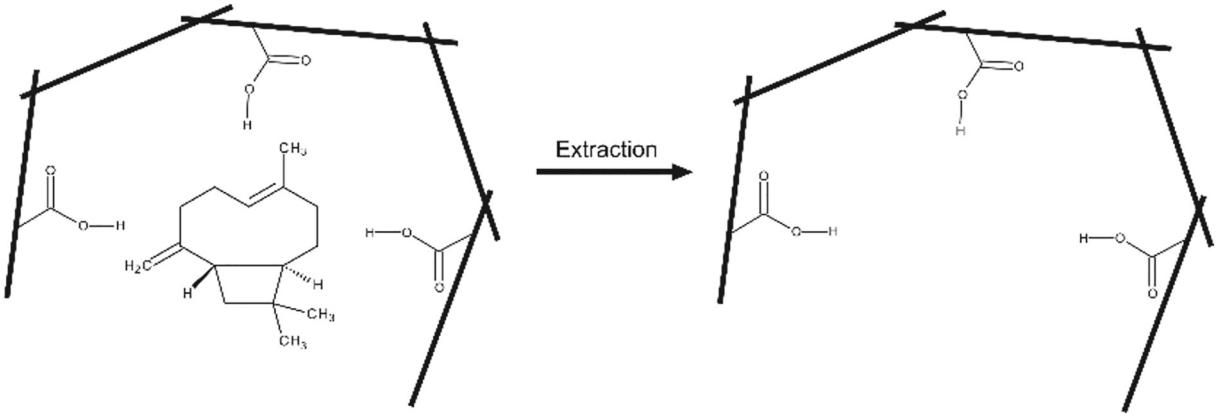

Fig. 1. Schematic representation of the functioning of MIP before and after template removal.

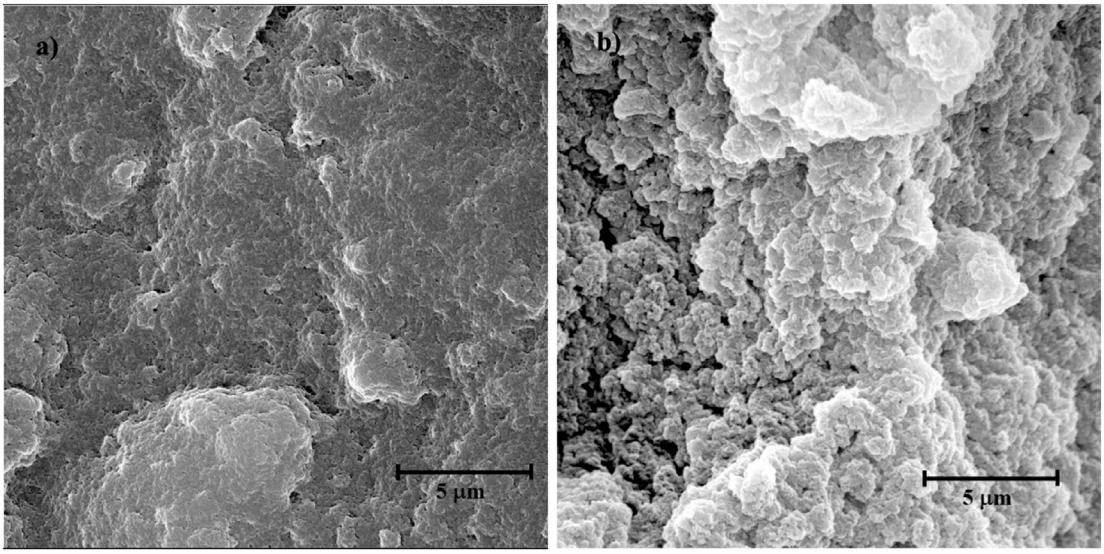

Fig. 2. SEM images of NIP (a) and MIP after template (β-caryophyllene) removal (b).

an incipient grain growth and non-porous structures relate to the synthesized NIP.

Otherwise, Fig. 2b) shows a well-defined grain boundary and a mean grain size of 100 nm. It is possible to observe an irregular morphology related to the typical porous structure that defines the MIP after the template removal [19].

3.2. Fourier transform infrared analysis

Fig. 3 shows a comparative study related to the infrared spectra of β-caryophyllene, NIP and MIP, before and after template removal, to identify the contributions to the vibrational spectra and to verify the functionality of the synthesized MIP. In the β-caryophyllene spectrum, itis possible to observe the vibrational strain (3071 cm^{-1}) of ═CH, and the asymmetric (2936 cm^{-1}) and the symmetric (2859 cm^{-1}) vibration stretching of the CH_2 group [20]. The small stretching at 1671 cm^{-1} refers to the absorption frequency of the alkyl group bonded directly to the ring double bond and the stretching C═C (1633 cm^{-1}) to the double bond that is outside of the terpene ring. It can also be observed the scissoring mode absorption band (1451 cm^{-1}) of the CH_2 bonded to the carbon of the double bond out of the ring [20,21] and the double peaks (1383 cm^{-1} and 1368 cm^{-1}) of the vibrations of symmetric CH_3 deformations attributed to the two methyl groups attached to the cyclobutane ring. Moreover, it is possible to detect an intense peak in the spectrum at 886 cm^{-1} characteristic of the ═C—H deformation of vibration out-of-plane [21].

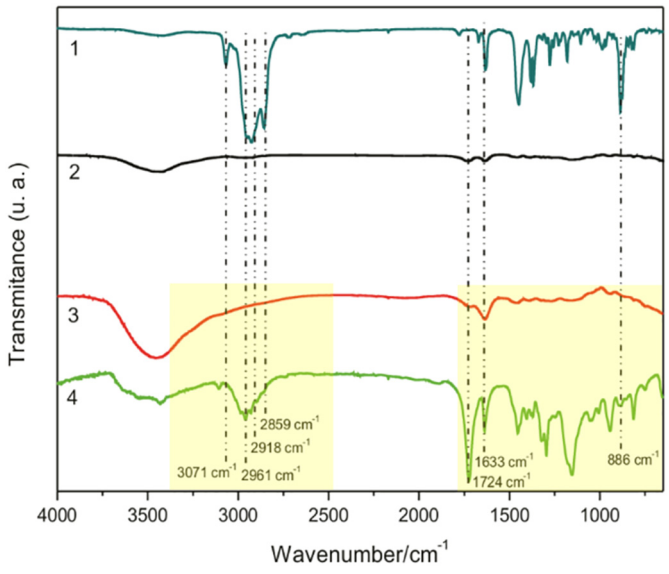

Fig. 3. FTIR spectra of β-caryophyllene (1), NIP (2), MIP after removal (3) and before removal of sesquiterpene β-caryophyllene (4). Yellows regions show details of the comparative FTIR spectra of MIP after and before removal of β-caryophyllene.

The NIP spectrum in Fig. 3 shows a wide band attributed to the OH stretching (3400 cm^{-1}), the asymmetric (2961 cm^{-1}), the symmetric (2918 cm^{-1}) stretching vibration typical of CH_2 and a small stretching at 1633 cm^{-1} due to the double bond (C═C). On the other hand, it can be observed a vibrational band relative to the carboxyl group (C═O) at 1724 cm^{-1} that in the acrylic acid (functional monomer) appears at 1670 cm^{-1} but after the polymerization process undergoes are shift [22,23].

Fig. 3 shows two yellow regions related to the comparison between FTIR spectra of MIP before and after template removal. The MIP spectrum after removal of the template has the similar spectral characteristics of NIP, which is constituted of poly(acrylic acid). However, the spectrum of MIP before template removal shows the contribution of molecular groups of β-caryophyllene. Thus, the characteristic small vibrational stretching at 3071 cm^{-1} related to the ═CH group was not found in the poly(acrylic acid) structure and, as previously discussed, this group is involved in the radical polymerization reaction, by which their incidence is only related to the template β-caryophyllene molecule.

On the other hand, the region of asymmetric (2936 cm^{-1}) and symmetric (2859 cm^{-1}) vibrations typical of CH_2 and the axial strain vibration bands of C═C groups were not detected in the MIP spectrum after template removal at testing the removing process of the template. These results are similar to the literature, where it was observed that after the extraction of the template from the polymeric matrix [24,25], a non-polar terpene class, as a sesquiterpene β-caryophyllene, form a non-covalent bonding with the polymeric matrix [26,27]. β-Caryophyllene does not have specific functional groups such as carboxyl or hydroxyl groups which could generate a strong interaction with the polymeric matrix. Thus, it is proposed that weak non-covalent interactions, such as Van der Waals, govern the interaction between the polymeric matrix and the template molecule [28,29].

3.3. Raman spectra analysis

Fig. 4 shows the Raman spectra of NIP (a) and MIP before (b) and after removal of the β-caryophyllene (c). The assignments of the Raman bands are summarized in Table A in Supplementary data.

Raman spectral signatures of both NIP and MIP before template removal are rather similar in the peaks position, although the intensities differ between them by 20%. This behavior can be related to the contribution of molecular groups of β-caryophyllene that have non-covalent interaction with the polymeric matrix [30]. The peaks located at 507 cm^{-1} and 603 cm^{-1} are due to the vibrations of CO_2 out of plate and CO_2 rotation, respectively. The peaks at 735 and 835 cm^{-1} are attributed to the C-COOH stretching vibrations; the peaks at 946 cm^{-1}, 1381 cm^{-1}, 1406 cm^{-1}, 1640 cm^{-1} and 1722 cm^{-1}correspond to vibration of the C—C stretching, C—H bending, δ(CH_2), C—H stretching and C—O stretching, respectively, presented in the carboxyl acid and acetyl groups [31–34]. The assignments of some modes, such as at 2902 cm^{-1}, 2932 cm^{-1}, 3046 cm^{-1} and 3110 cm^{-1} are associated to the CH stretching and CH_2 bond, and C—H and CH_2 symmetrical vibrations and correspond to the carbonyl group present in the poly(acrylic acid).

On the other hand, the peak located at 2857 cm^{-1} appears only in the spectrum of MIP before the β-caryophyllene removal, showing that the template was removed from the polymeric matrix. This peak corresponds to the CH_3 symmetrical stretching mode and may be associated with saturated carbon [35].

3.4. XPS analysis

For in-depth analysis of the surface chemical species present in the different states of operation of MIP, high resolution XPS spectra were recorded. High-resolution C1s and O1s XPS spectra are shown in Fig. 5 for NIP and MIP before and after template removal. They were fitted with three peaks, using symmetric Voigt curves based on a convolution of Gaussian and Lorentzian curves [36].

In the deconvoluted C1s XPS spectra, the first peak was assigned to the C—C bonds in the aliphatic chain of the poly(acrylic acid) present in the polymeric matrix, the second one to the C—O bond and the third to carbonyl, C═O, present in the functional group of acrylic acid monomer [37,38]. In the O1s XPS spectra, the first peak was assigned to the C—O bonds, the second to carbonyl, C═O and the third to adsorbed water [38]. The binding energy and atomic percentage values of the chemical species present are given in Table B in Supplementary data file.

Fig. 5a and b shows the C1s XPS spectra for NIP, i.e. for poly(acrylic acid) and for MIP after the removal of β-caryophyllene. It was observed a great similarity in the shape of the spectra and, also, no shift in the binding energy due to the great similarity in the chemical environment at the C 1s core level after the removal of β-caryophyllene. Thus, the ratio of atomic percentages between C—C and C—O for the NIP and MIP after removal of β-caryophyllene is very close: 1.96 and 2.02, respectively, indicating that the chemical environment around the carbon and oxygen atoms did not change with the absence of the β-caryophyllene molecule in the polymeric matrix.

Fig. 5b and c shows the XPS spectra of the C1s for the MIP before the removal of the β-caryophyllene molecule and for the MIP after the removal of the β-caryophyllene molecule. Here, it is possible to notice an accentuated difference in the peak intensities attributed to C—C bond due to the presence of sp2 and sp3 carbon atoms present in the β-caryophyllene structure. β-Caryophyllene is a molecule which exhibits in its bicyclic structure alkyl groups (–CH, $–CH_2$, $–CH_3$ and $=CH_2$) that form non-covalent intermolecular interactions of the dispersion forces type (also known as London forces), which are weak intermolecular interactions that happen by the phenomenon of induction of the dipole moment of the electronic cloud [39].

The values of the atomic percentages of the C—C and C—O bonds show a significant increase of 2.02 (absence of β-caryophyllene) to a value of 2.63 (presence of β-caryophyllene) strongly indicating the contribution of the sp2 and sp3 carbon atoms of the β-caryophyllene molecule. It is known that the intermolecular interaction between the β-caryophyllene and the active cavities formed within the MIP, mainly by the carbonyl group, C═O, occurs by permanent dipole – induced dipole; as it is a very weak interaction it is not possible to assign an

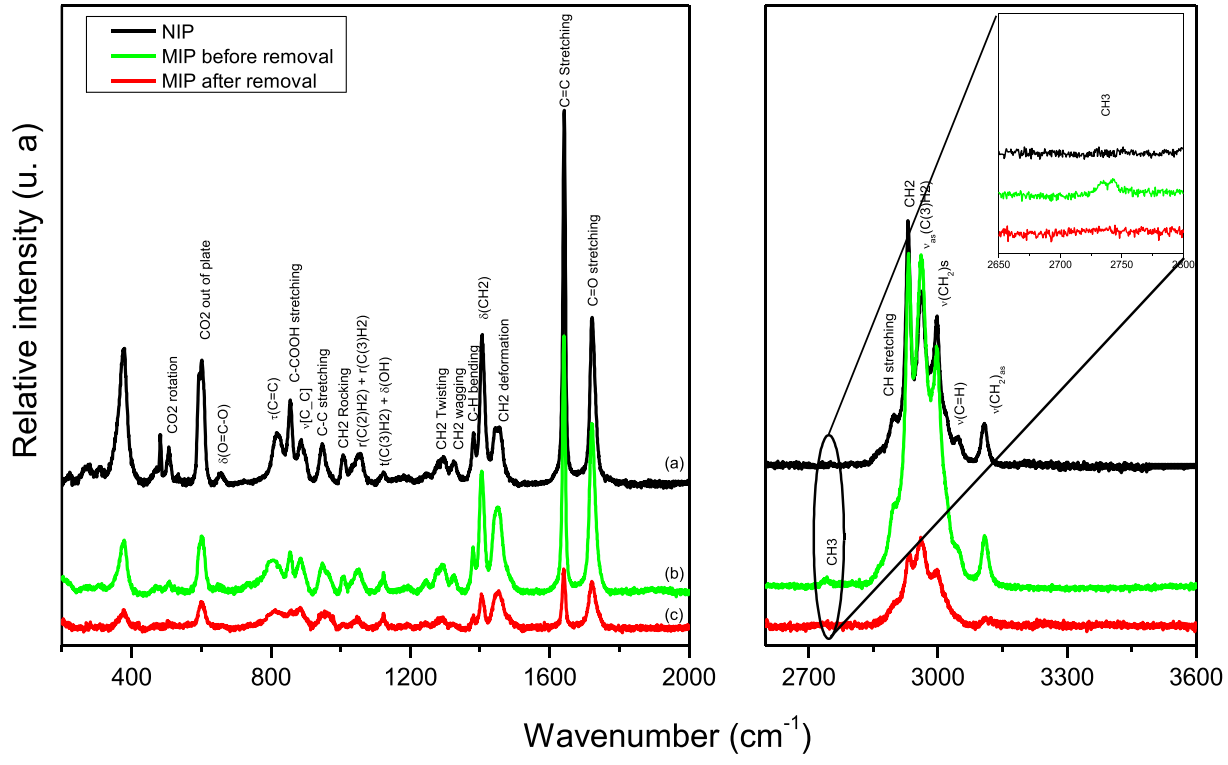

Fig. 4. Raman spectra of NIP (a), MIP before (b) and after removal (c) of the template β-caryophyllene.

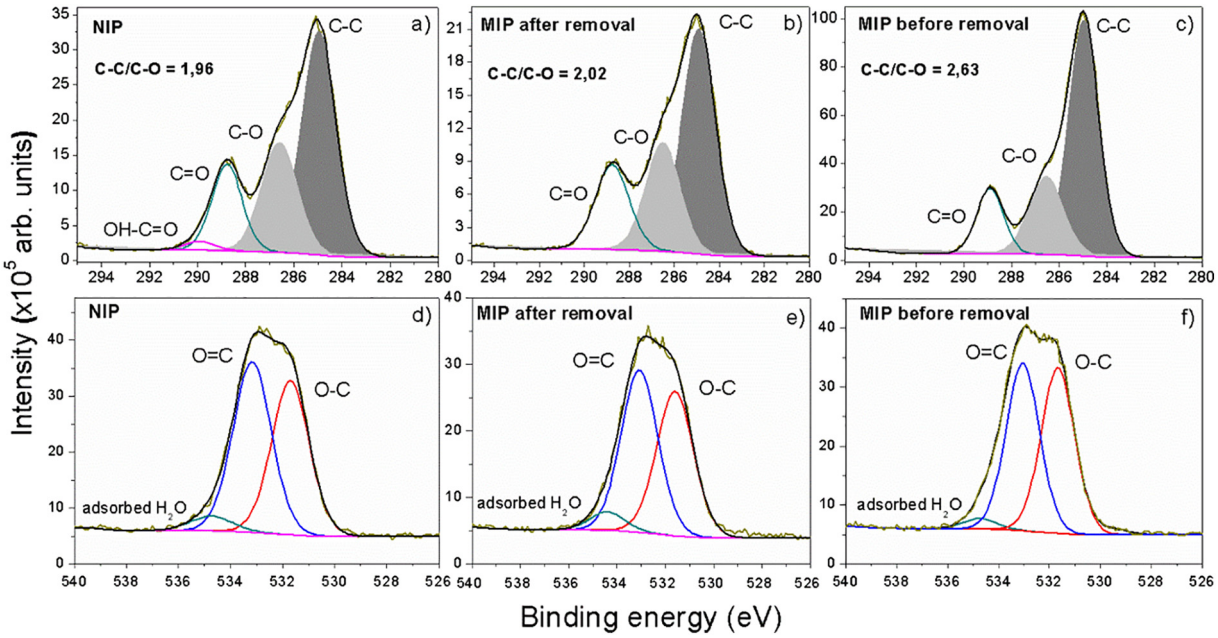

Fig. 5. High-resolution XPS spectra of C1s and O1s core levels for NIP (a and d), MIP before (b and e) and after (c and f) removal of β-caryophyllene.

increase of BE to this interaction, only as a consequence of the presence of carbon atom sp2, $=CH_2$ of β-caryophyllene [40–42]. The O1s core level did not show any significant changes with the presence or absence of the β-caryophyllene as molecular template. In summary, such results corroborate with those presented by RAMAN and FTIR spectroscopies.

3.5. Voltammetric analyses

Sesquiterpene β-caryophyllene is a non-polar molecule that presents low electroactivity. Because of this it was considered the indirect detection method for measuring the electrochemical response of the modified carbon electrode with NIP and MIP before and after template removal. Fig. 6 shows comparative cyclic voltammograms related to modified CPE. First, the CPE was built using a synthesized MIP that was macerated and treated to the removed template as described above. Then, the CPE modified with MIP after template removal was placed in β-caryophyllene solution (7.5×10^{-7} M) for 5 min to the reabsorbed template. The voltammograms for modified CPE with NIP and MIP before and after the removal of the template were acquired using electrolyte solution of $[K_3[Fe(CN)_6]/K_4[Fe(CN)_6]$ (5 mM) and KCl (0.2 M).

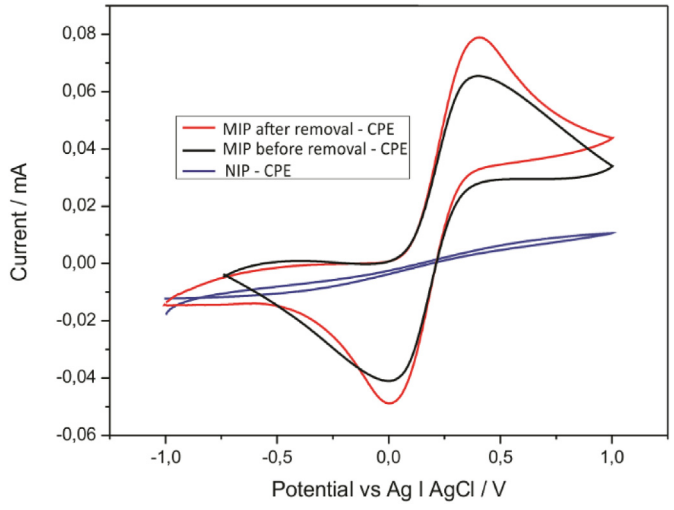

Fig. 6. Comparative cyclic voltammograms performed in $K_3[Fe(CN)_6]/K_4[Fe(CN)_6$ (5 mM) in KCl (0.2 M) for modified CPE with NIP and MIP before and after the template removal.

The voltammogram using the CPE modified with NIP did not present the characteristics of the $K_3[Fe(CN)_6]/K_4[Fe(CN)_6$ redox pair, showing a higher resistivity if compared with the voltammograms of MIP before and after template removal. This behavior can be attributed to the polymeric structure of NIP that does not present the imprinted cavities of the template molecule where the diffusion of the $K_3[Fe(CN)_6]/K_4[Fe(CN)_6$ redox pair occurs. The respective voltammograms of MIP before and after template removal show the characteristics of the $K_3[Fe(CN)_6]/K_4[Fe(CN)_6$ pair. Thus, the polymeric matrix of MIP submitted to the process of template removal provides cavities that enable the diffusional process of the $K_3[Fe(CN)_6]/K_4[Fe(CN)_6$ species and the charge transfer reactions on the electrode interface [43].

The modified CPE with MIP after template removal was immersed in the β-caryophyllene solution for 5 min and the obtained cyclic voltammograms showed the $K_3[Fe(CN)_6]/K_4[Fe(CN)_6$ redox pair, despite a decreasing of the current of the redox process was observed. This decreasing of the current can be explained by the reabsorbed templates molecules, which occupy the cavities in the polymeric matrix of MIP that limit the diffusion of electrolyte species and the charge transfer.

3.6. Determination of sesquiterpene β-caryophyllene

Fig. 7A shows the square wave voltammograms related to the determination of β-caryophyllene using modified CPE with MIP after template removal. For the detection study modified CPE was immersed in solutions containing different concentrations of β-caryophyllene.

The SWV shows the decrease of the current of the oxidation peak when the concentration of β-caryophyllene was increased in the solution. As explained above, the cavities in the polymeric matrix of MIP are being occupied when the electrode is incubated in β-caryophyllene solution and this process is increased as the electrode is exposed to higher concentrations of β-caryophyllene. The current of the oxidation peak decreases with the increase of the β-caryophyllene concentration from 1.5×10^{-7}–7.5×10^{-7} M with a correlation coefficient of 0.9916 (Fig. 7B). Analogous behavior was related by X. Kan et al. and X.L. Jing Luo et al. in the bovine hemoglobin detection [44,45] and also reported in the studies for the determination of testosterone, epigallocatechin-3-gallate in green tea and 4-nonphenol [25,46,47].

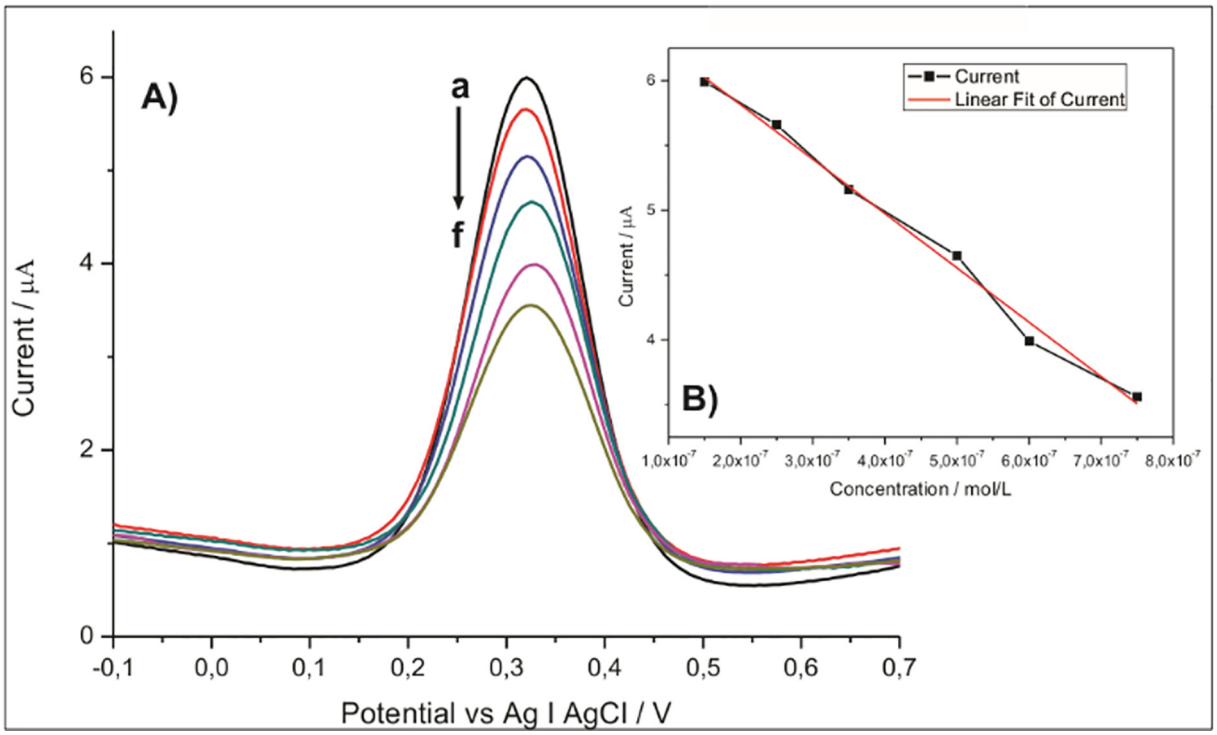

Fig. 7. A) The SWV with modified CPE with MIP after template removal in different concentrations of their respective standards. The concentration of β-caryophyllene in curves a–f was as follows: 1.5×10^{-7}, 2.5×10^{-7}, 3.5×10^{-7}, 5×10^{-7}, 6×10^{-7} and 7.5×10^{-7} M, respectively. B) The linear relationship between the peak current and the concentration of β-caryophyllene in a range of 1.5×10^{-7}–7.5×10^{-7} M. The initial and final potentials were set as −0.1 V and +0.7 V, respectively.

4. Conclusion

The development of a novel sensor for the detection of sesquiterpene β-caryophyllene based on modified CPE with MIP was presented. The synthesized NIP and MIP was structurally characterized showing the formation of porous structure in the MIP after removal of the β-caryophyllene. The spectroscopic characterization made possible to demonstrate the functional features of the synthesized MIP before and after extraction of the template. The electrochemical techniques such as CV allowed to deepen into the mechanisms of molecular recognition and the electroactive characteristics of β-caryophyllene. The detection of β-caryophyllene was performed through the SWV that enabled the detection in a concentration range between 1.5 and 7.5×10^{-7} M with the correlation coefficient of 0.9916. These results showed the great potential of monitoring the content of the sesquiterpene β-caryophyllene in technological processes and for predicting the quality of extracts, oils, and resins of plants.

Acknowledgments

We would like to thank CAPES (Coordination for the Improvement of Higher Education Personnel) and FAEPAM (Amazonas State Research Support Foundation) for financial support. M.L.M.R. thanks CNPq and CT-INFRA-FINEP for financial support.

Disclosure

The authors declare no competing financial interest.

Appendix A. Supplementary data

Supplementary data to this article can be found online at https://doi.org/10.1016/j.saa.2019.03.097.

References

[1] M.J. Chavan, P.S. Wakte, D.B. Shinde, Analgesic and anti-inflammatory activity of Caryophyllene oxide from Annona squamosa L. bark, Phytomedicine 17 (2010) 149–151, https://doi.org/10.1016/j.phymed.2009.05.016.
[2] A.C. Goren, F. Piozzi, E. Akcicek, T. Kılıc, C. Sema, W.N. Setzer, E. Moziog, Essential oil composition of twenty-two Stachys species (mountain tea) and their biological activities, Phytochem. Lett. 4 (2011) 448–453, https://doi.org/10.1016/j.phytol.2011.04.013.
[3] S. Cheng, C. Wu, H. Chang, Y. Kao, S. Chang, Antitermitic and antifungal activities of essential oil of Calocedrus formosana leaf and its composition, J. Chem. Ecol. 30 (2004) 1957–1967.
[4] L. Saulo, P.M.S. Figueiredo, T. Yano, Chemotherapeutic potential of the volatile oils from Zanthoxylum rhoifolium Lam leaves, Eur. J. Pharmacol. 576 (2007) 180–188, https://doi.org/10.1016/j.ejphar.2007.07.065.
[5] A. Di, G. Mazzanti, F. Carbone, P. Hrelia, F. Maffei, Inhibition by β-caryophyllene of ethyl methanesulfonate-induced clastogenicity in cultured human lymphocytes, Mutat. Res. Genet. Toxicol. Environ. Mutagen. 699 (2010) 23–28, https://doi.org/10.1016/j.mrgentox.2010.04.008.
[6] J. Legault, A. Pichette, Potentiating Effect of β-Caryophyllene on Anticancer Activity of α-Humulene, Isocaryophyllene and Paclitaxel, 2007 1643–1647, https://doi.org/10.1211/jpp.59.12.0005.
[7] G.M. Carla Ghelardini, Giuseppe Salvatore Nicoletta, Local anaesthetic activity of the essential oil of Lavandula angustifolia, Planta Med. (1999) 700–703.
[8] A. Shafaghat, Antibacterial activity and GC/MS analysis of the essential oils from flower, leaf and stem of Origanum vulgare ssp. viride growing wild in north-west Iran, Nat. Prod. Commun. 20 (2015).
[9] F.B. Carneiro, I.D. Júnior, P.Q. Lopes, R.O. Macêdo, Artigo Variação da quantidade de β-cariofileno em óleo essencial de Plectranthus amboinicus (Lour.) Spreng., Lamiaceae, sob diferentes condições de cultivo, vol. 20, 2010 600–606.
[10] L.F. Salomé-Abarca, J. Van Der Pas, H.K. Kim, G.A. Van Uffelen, P.G.L. Klinkhamer, Y. Hae, Metabolic discrimination of pine resins using multiple analytical platforms, Phytochemistry 155 (2018) 37–44.
[11] L.I. Andersson, Efficient sample pre-concentration of bupivacaine from human plasma by solid-phase extraction on molecularly imprinted polymers, Analyst 125 (2000) 1515–1517, https://doi.org/10.1039/b005386o.
[12] K. Nilsson, J. Lindell, O. Norrlöw, B. Sellergren, Imprinted polymers as antibody mimetics and new affinity gels for selective separations in capillary electrophoresis, J. Chromatogr. A 680 (1994) 57–61, https://doi.org/10.1016/0021-9673(94)80052-9.
[13] W. Liu, Y. Guo, J. Luo, J. Kou, H. Zheng, B. Li, Z. Zhang, A molecularly imprinted polymer based a lab-on-paper chemiluminescence device for the detection of dichlorvos, Spectrochim. Acta A Mol. Biomol. Spectrosc. 141 (2015) 51–57, https://doi.org/10.1016/J.SAA.2015.01.020.

[14] A. Khataee, J. Hassanzadeh, E. Kohan, Specific quantification of atropine using molecularly imprinted polymer on graphene quantum dots, Spectrochim. Acta A Mol. Biomol. Spectrosc. 205 (2018) 614–621, https://doi.org/10.1016/J.SAA.2018.07.088.
[15] E.H.M. Koster, C. Crescenzi, W. Den Hoedt, K. Ensing, G.J. De Jong, Fibers coated with molecularly imprinted polymers for solid-phase microextraction, Anal. Chem. 73 (2001) 3140–3145, https://doi.org/10.1021/ac001331x.
[16] P.T.-B.M.C. Blanco-López, M.J. Lobo-Castañón, A.J. Miranda-Ordieres, Voltammetric sensor for vanillylmandelic acid based on molecularly imprinted polymer-modified electrodes, Biosens. Bioelectron. 18 (2003).
[17] C.C. Hwang, W.C. Lee, Chromatographic characteristics of cholesterol-imprinted polymers prepared by covalent and non-covalent imprinting methods, J. Chromatogr. A 962 (2002) 69–78, https://doi.org/10.1016/S0021-9673(02)00559-9.
[18] S. Pardeshi, R. Dhodapkar, A. Kumar, Studies of the molecular recognition abilities of gallic acid-imprinted polymer prepared using a molecular imprinting technique, Adsorpt. Sci. Technol. 30 (2012) 23–34, https://doi.org/10.1260/0263-6174.30.1.23.
[19] X. Feás, C.A. Fente, S.V. Hosseini, J.A. Seijas, B.I. Vázquez, C.M. Franco, A. Cepeda, Use of acrylic acid in the synthesis of molecularly imprinted polymers for the analysis of cyproheptadine, Mater. Sci. Eng. C 29 (2009) 398–404, https://doi.org/10.1016/j.msec.2008.08.011.
[20] J. Kühn-institut, H. Schulz, M. Baranska, Identification and quantification of valuable plant substances by IR and Raman spectroscopy identification and quantification of valuable plant substances by IR and Raman spectroscopy, Vib. Spectrosc. (2007) https://doi.org/10.1016/j.vibspec.2006.06.001.
[21] H. Liu, G. Yang, Y. Tang, D. Cao, T. Qi, Y. Qi, G. Fan, Physicochemical characterization and pharmacokinetics evaluation of β-caryophyllene/β-cyclodextrin inclusion complex, Int. J. Pharm. 450 (2013) 304–310.
[22] C. Chemistry, CH_2, (n.d.).
[23] R. Ravichandran, S. Nanjundan, N. Rajendran, Effect of benzotriazole derivatives on the corrosion of brass in NaCl solutions, Appl. Surf. Sci. 236 (2004) 241–250, https://doi.org/10.1016/j.apsusc.2004.04.025.
[24] B. Khadro, C. Sanglar, A. Bonhomme, A. Errachid, N. Jaffrezic-Renault, Molecularly imprinted polymers (MIP) based electrochemical sensor for detection of urea and creatinine, Procedia Eng. 5 (2010) 371–374, https://doi.org/10.1016/j.proeng.2010.09.125.
[25] A. Betatache, F. Lagarde, C. Sanglar, A. Bonhomme, D. Leonard, N. Jaffrezic-Renault, Gold electrodes modified with molecular imprinted acrylate polymer for impedimetric determination of testosterone, Sens. Transducers 27 (2014) 92–99.
[26] L.E.I. Ye, K. Mosbach, The technique of molecular imprinting — principle, state of the art, and future aspect, J. Incl. Phenom. Macrocycl. Chem. 41 (2001) 107–113, https://doi.org/10.1023/A:1014498404292.
[27] L. Ye, K. Mosbach, Molecular imprinting: synthetic materials as substitutes for biological antibodies and receptors, Chem. Mater. 20 (2008) 859–868, https://doi.org/10.1021/cm703190w.
[28] B. Chen, C. Liu, K. Hayashi, Selective terpene vapor detection using molecularly imprinted polymer coated au nanoparticle LSPR sensor, IEEE Sensors J. 14 (2014) 3458–3464, https://doi.org/10.1109/JSEN.2014.2346187.
[29] H. Asanuma, T. Hishiya, M. Komiyama, Efficient separation of hydrophobic molecules by molecularly imprinted cyclodextrin polymers, J. Incl. Phenom. 50 (2004) 51–55, https://doi.org/10.1007/s10847-003-8838-4.
[30] B.S. Batlokwa, J. Mokgadi, T. Nyokong, N. Torto, Optimal template removal from molecularly imprinted polymers by pressurized hot water extraction, Chromatographia 73 (2011) 589–593, https://doi.org/10.1007/s10337-010-1884-3.
[31] H. Nomura, M. Nagasawa, S. Koda, Biophys. Chem. 18 (1983) 361–367.
[32] J. Dong, Y. Ozaki, K. Nakashima, Infrared, Raman, and near-infrared spectroscopic evidence for the coexistence of various hydrogen-bond forms in poly(acrylic acid), Macromolecules 9297 (1997) 1111–1117.
[33] C. Murli, Y. Song, Pressure-induced polymerization of acrylic acid: a Raman spectroscopic study, J. Phys. Chem. B (2010) 9744–9750.
[34] J. Koo, J. Kim, H. Lee, H. Chung, Y. Lee, W. Yi, D. Sohn, Formation and characterization of poly(acrylic acid) on silica particles irradiated by γ-ray radiation, Macromol. Res. 20 (2012) 138–142, https://doi.org/10.1007/s13233-012-0078-2.
[35] R. These, Compounds Containing the Carbonyl Group, 1900 3.
[36] V. Jain, M.C. Biesinger, M.R. Linford, The Gaussian-Lorentzian sum, product, and convolution (Voigt) functions in the context of peak fitting X-ray photoelectron spectroscopy (XPS) narrow scans, Appl. Surf. Sci. 447 (2018) 548–553, https://doi.org/10.1016/J.APSUSC.2018.03.190.
[37] L.J. Ward, W.C.E. Schofield, J.P.S. Badyal, Atmospheric Pressure Plasma Deposition of Structurally Well-defined Polyacrylic Acid Films, 2003 1466–1469.
[38] P. Louette, F. Bodino, J. Pireaux, Poly(acrylic Acid) (PAA) XPS Reference Core Level and Energy Loss Spectra, 2005https://doi.org/10.1116/11.20050905.
[39] N. Marom, A. Tkatchenko, M. Rossi, V.V. Gobre, O. Hod, M. Sche, L. Kronik, Dispersion Interactions with Density-Functional Theory : Benchmarking Semiempirical and Interatomic Pairwise Corrected Density Functionals, 2011 3944–3951.
[40] I. Novak, B. Kova˜, Photoelectron Spectroscopy of Natural Products: Terpenes, 61, 2005 277–280, https://doi.org/10.1016/j.saa.2004.04.015.
[41] S. Hu, J. Yu, E.Y. Zeng, A Theoretical Study on UV-spectroscopy, Electronic Structure and Reactivity Properties of Sesquiterpenes, 2010https://doi.org/10.5194/acpd-10-24325-2010.
[42] M.S. El-shall, G.M. Daly, D. Wright, Experimental and theoretical study of benzene $(acetonitrile)_n$ clusters, n = 1–4, J. Chem. Phys. (2002) 10253, https://doi.org/10.1063/1.1476317.
[43] C. Ricardo, T. Tarley, M. Del, P. Taboada, L. Tatsuo, Polímeros biomiméticos em química analítica. Parte 2: aplicações de mip ("molecularly imprinted polymers") no desenvolvimento de sensores químicos, 28, 2005 1087–1101.
[44] X. Kan, Z. Xing, A. Zhu, Z. Zhao, G. Xu, C. Li, H. Zhou, Molecularly imprinted polymers based electrochemical sensor for bovine hemoglobin recognition, Sensors Actuators B Chem. 168 (2012) 395–401, https://doi.org/10.1016/j.snb.2012.04.043.
[45] X.L. Jing Luo, Sisi Jiang, The electrochemical sensor for bovine hemoglobin based on a novel graphene-molecular imprinted polymers composite as recognition element, Sensors Actuators B. Chem. 203 (2014) 782–789, https://doi.org/10.1016/j.snb.2012.04.043.
[46] Y. Duan, X. Luo, Y. Qin, H. Zhang, G. Sun, X. Sun, Y. Yan, Determination of epigallocatechin-3-gallate with a high-efficiency electrochemical sensor based on a molecularly imprinted poly(o-phenylenediamine) film, J. Appl. Polym. Sci. 129 (2013) 2882–2890, https://doi.org/10.1002/app.39002.
[47] N. Hong-Jun Chen, W.R. Zhao-Hui Zhang, Rong Cai, Xing Chen, Yu-Nan Liu, S.-Z. Yao, Molecularly imprinted electrochemical sensor based on amine group modified graphene covalently linked electrode for 4-nonylphenol detection, Talanta 115 (2013) 222–227, https://doi.org/10.1039/c3an00146f.